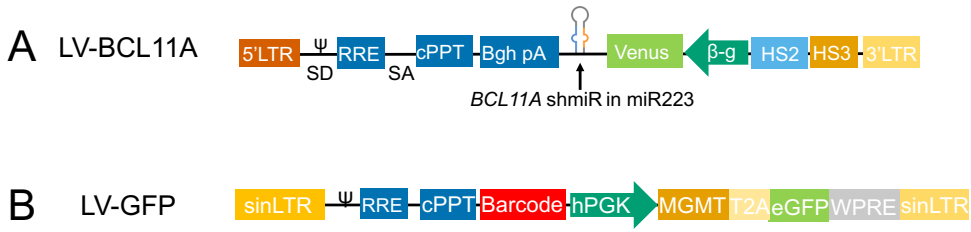


Figure S1. Diagrams of lentiviral vector constructs. (A) LV-BCL11A, LV-LCR-miR223 BCL11A lentiviral vectors with shmiR targeting BCL11A, (B) LV-GFP, pCCLsincPPT-PGK-MGMT-P140K-GFP-WPRE lentivirus vector consisting of a human PGK promoter regulating green fluorescent protein (GFP) and synthetic barcode fragments.

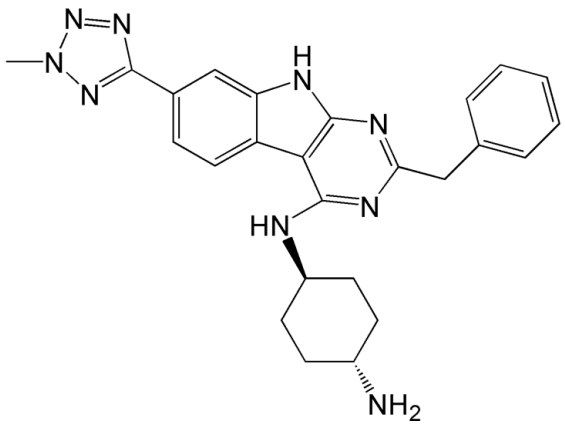


Figure S2. Chemical structure of UM171.

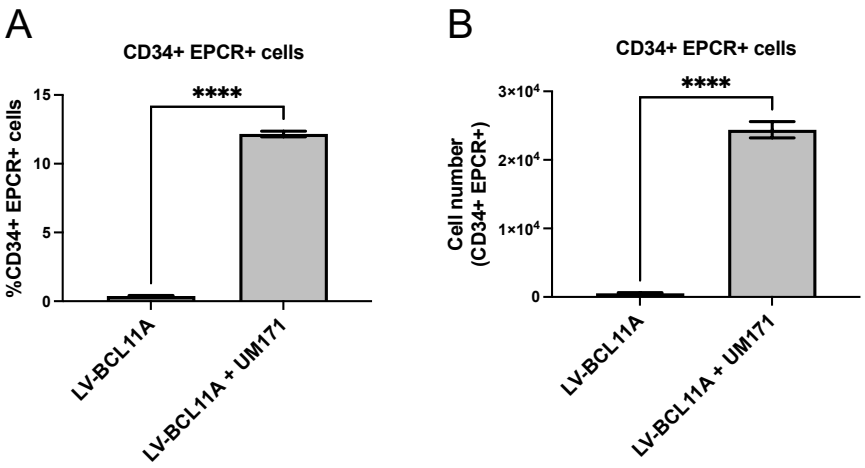


Figure S3. UM171 enhances the *in vitro* expansion of CD34+ cells from SCD patients. (A) The percentage of CD34+ EPCR+ cells and (B) CD34+ EPCR+ absolute cell numbers after transduction in the presence or absence of UM171. Data represent mean ± SD, n = 3, three independent experiments from different SCD patients' cells. **** $p < 0.0001$.

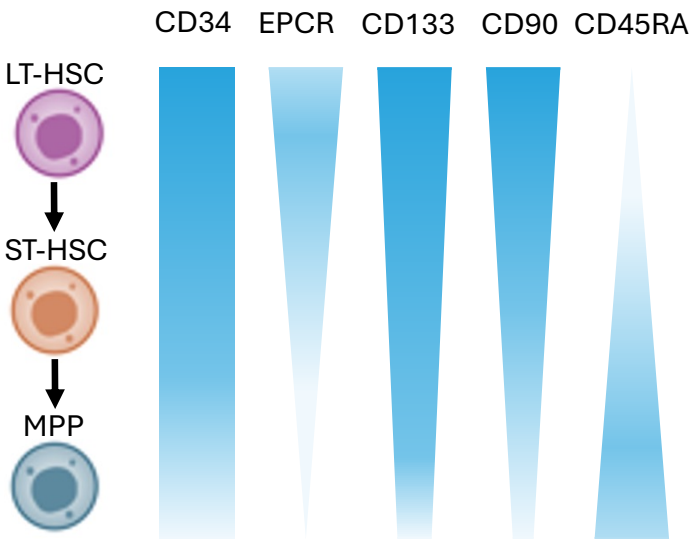


Figure S4. Surface markers CD34, EPCR, CD133, CD90, CD45RA expressions of human HSCs at different stages of differentiation.

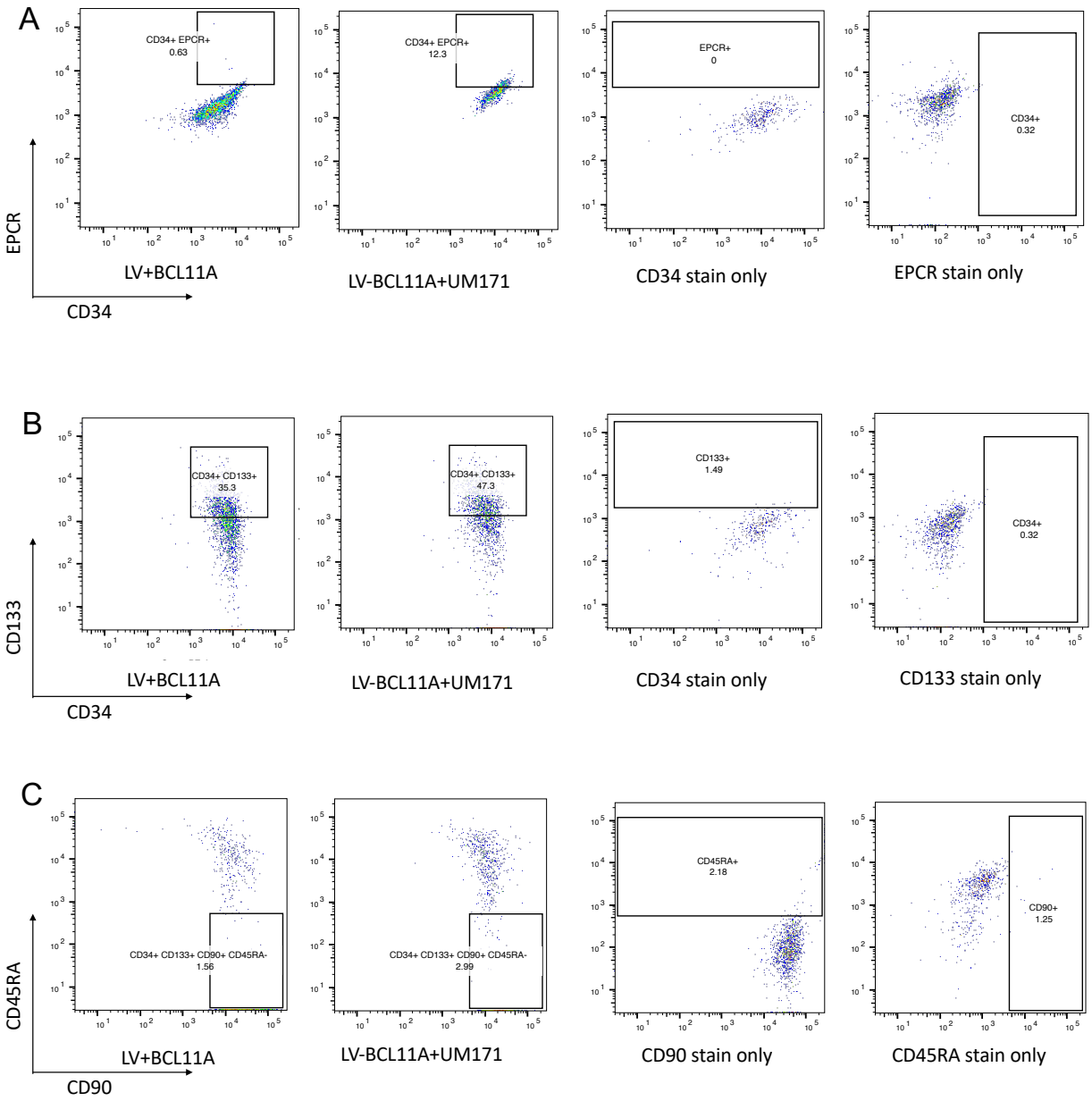


Figure S5. Representative flow cytometry analysis of (A) CD34+ EPCR+, (B) CD34+ CD133+ and (C) CD34+ CD133+ CD90+ CD45RA- population of SCD CD34+ cells after 7 days culture presence or absence of UM171.

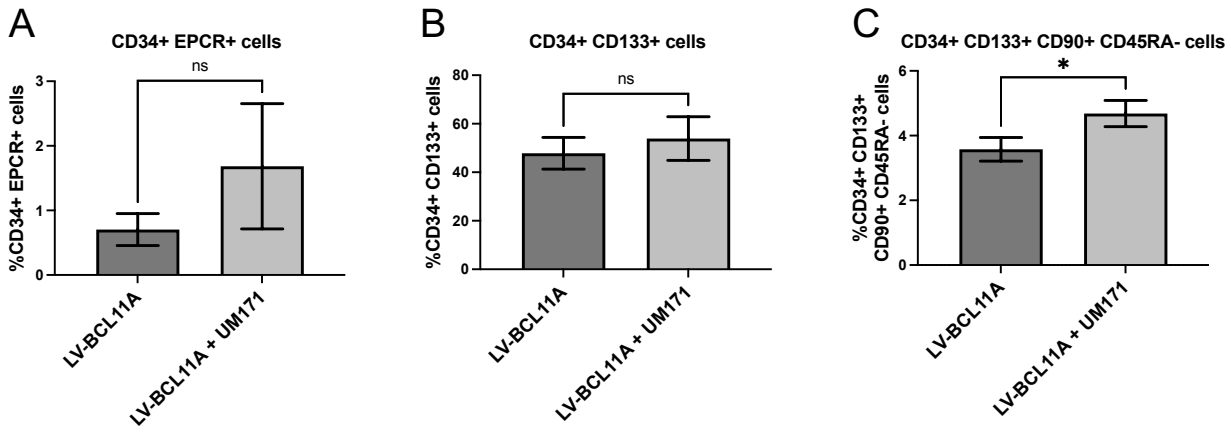


Figure S6. The percentage of (A) CD34+ EPCR+ cells, (B) CD34+ CD133+ and (C) CD34+ CD133+ CD90+ CD45RA- after transduction in the presence or absence of UM171 for 3 days. Data represent mean ± SD, n = 3, three independent experiments from different SCD patient cells. * $p < 0.05$.

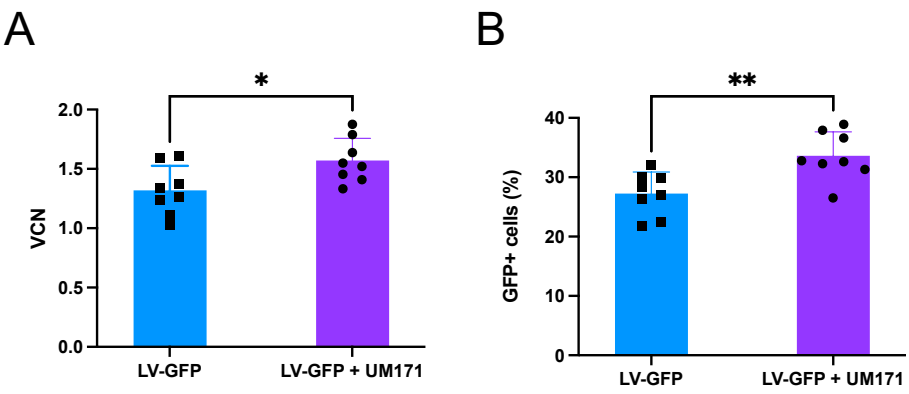


Figure S7. UM171 increases transduction efficiency of CD34+ cells from SCD patients analyzed *in vitro*. (A) VCN and (B) percentage of GFP+ cells of SCD CD34+ cells transduced with LV-GFP in the presence or absence of UM171 for three days. Data represent mean ± SD, n = 8, each data point represents an individual experiment. *$p < 0.05$, **$p < 0.01$.

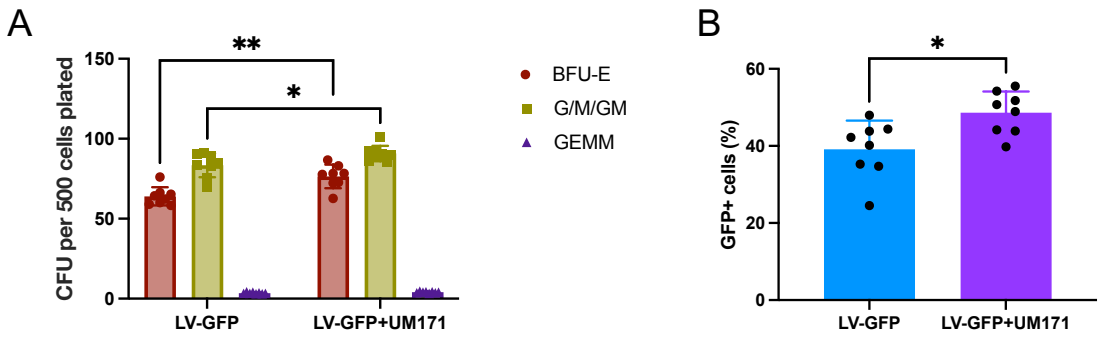


Figure S8. UM171 increases progenitor numbers in CFU assays of CD34+ cells from SCD patients. (A) CFU clones counts per 500 CD34+ cells plated. (B) %GFP+ CFU cells after 14 days CFU culture of 500 CD34+ cells transduced with LV-GFP in presence or absence of UM171. Data represent mean ± SD, n = 8, eight independent replicates from different patients' cells. *p < 0.05, **p < 0.01.

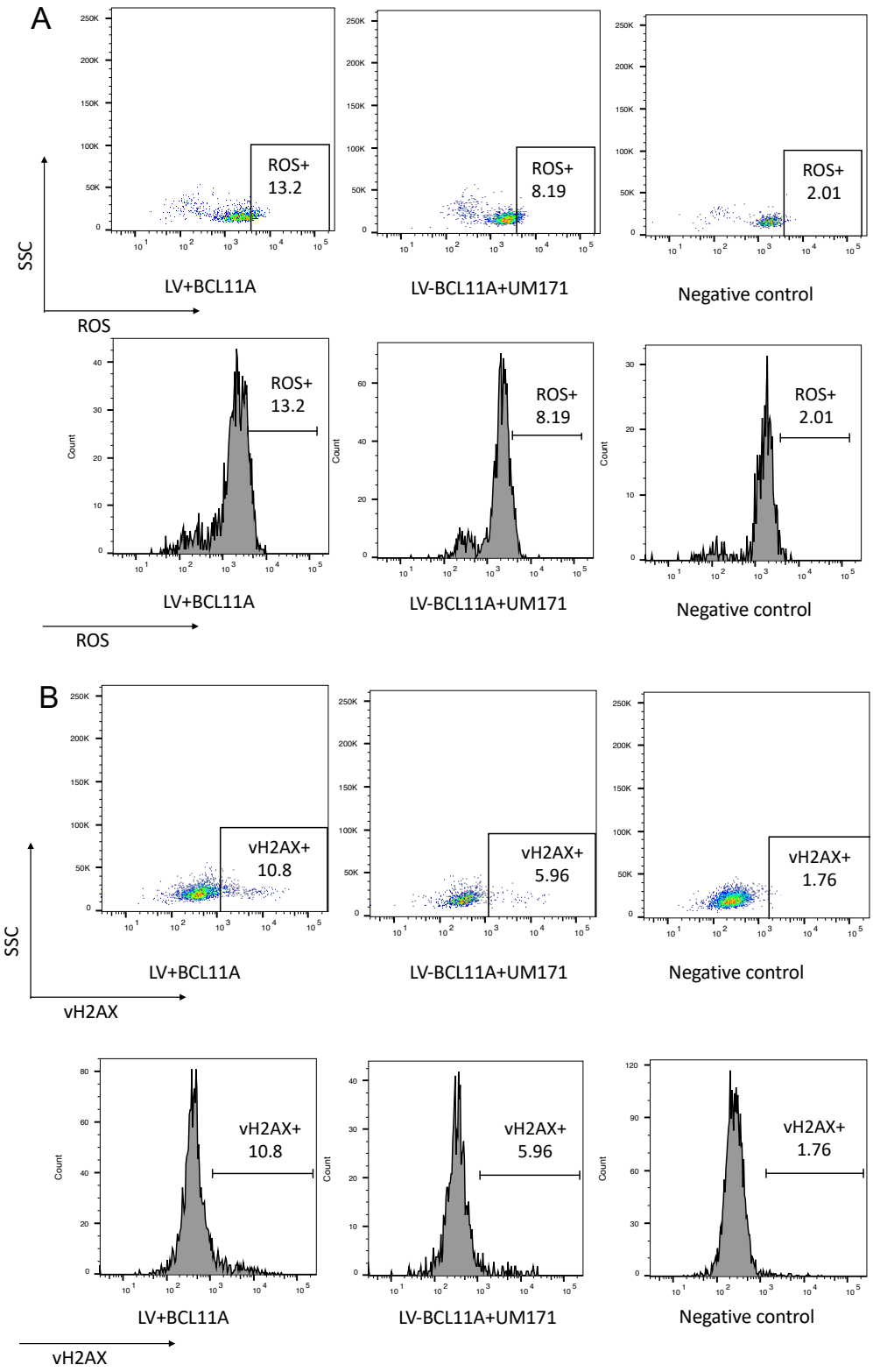


Figure S9. Representative flow cytometry analysis of (A) ROS and (B) $\gamma$H2AX of SCD CD34+ cells after 7 days culture presence or absence of UM171.

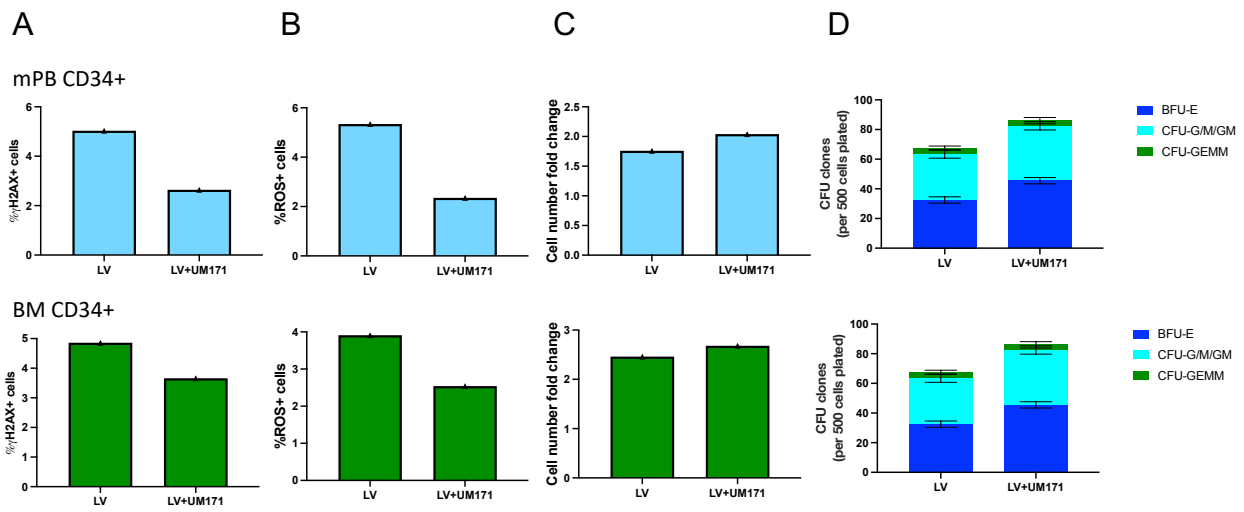


Figure S10. *In vitro* expansion of SCD CD34+ cells from different source SCD patients with or without UM171. (A) DNA damage was assessed by the level of $\gamma$H2AX staining, (B) assessment the level of ROS+ cells, (C) total cell number fold change and (D) CFU clones after transduction in the presence or absence of UM171.

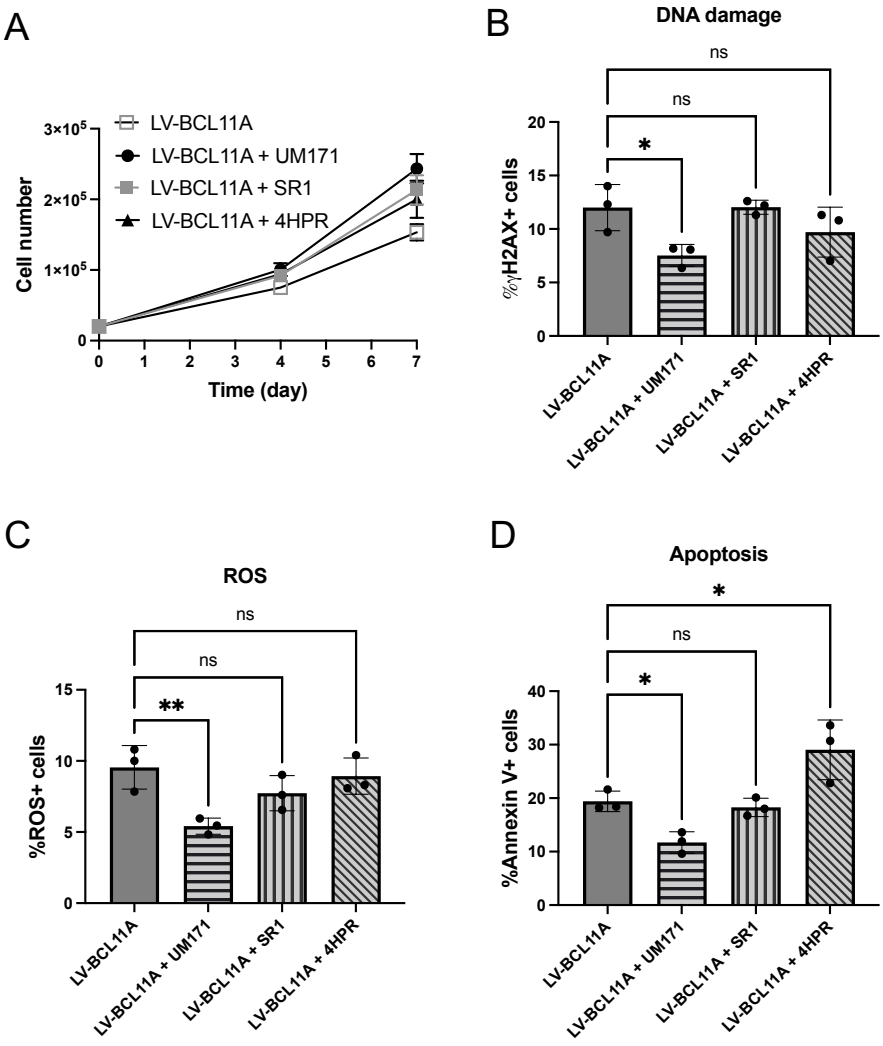


Figure S11. Comparative effects of UM171, SR1 and 4HPR on CD34+ from SCD patients during *in vitro* transduction. (A) Total cell numbers of CD34+ cells transduced with LV-BCL11A in presence of UM171, SR1 or 4HPR. (B) DNA damage was assessed by the level of $\gamma$H2AX staining. (C) Assessment of the level of ROS+ cells, and (D) the percentage of Annexin V+ cells after transduction in the presence of UM171, SR1 or 4HPR. Read outs after 7 days in culture. Data represent mean ± SD, n = 3, three independent experiments from different SCD patients' cells. *p < 0.05, **p < 0.01.

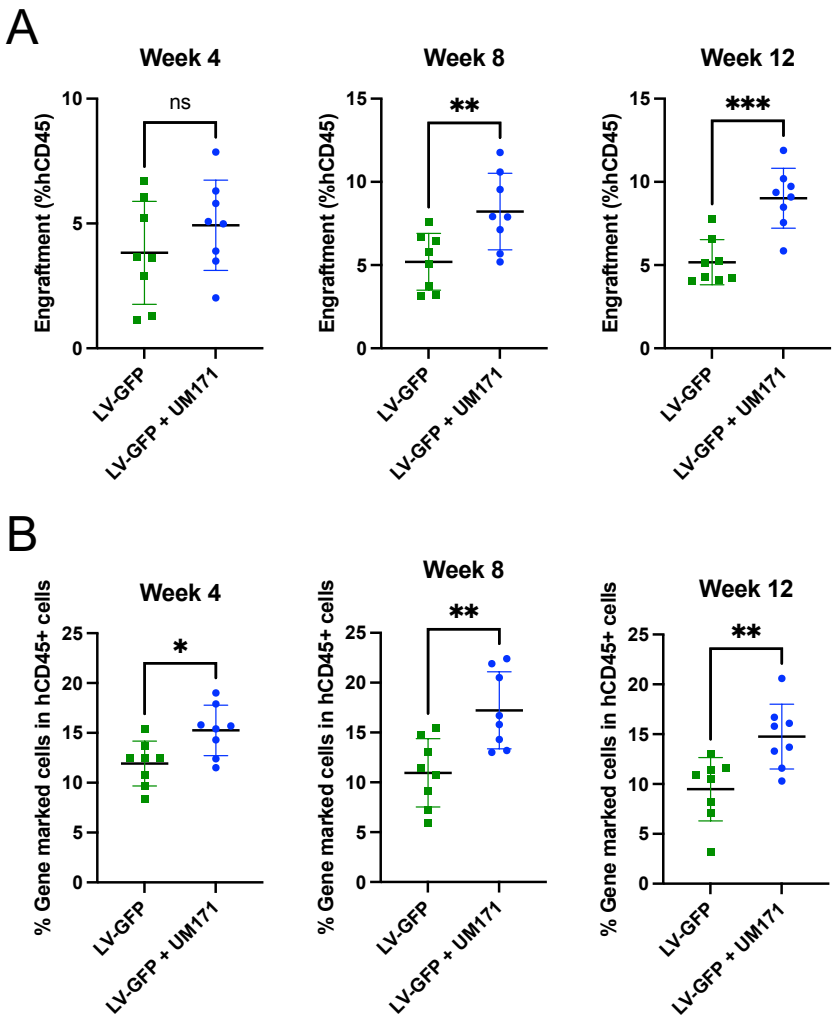


Figure S12. UM171 increases engraftment of CD34+ cells from SCD patients transduced with LVV expressing GFP in NBSGW mice. (A) Engraftment of cells and (B) gene-marked cells in PB at weeks 4-12 after NBSGW mice were transplanted with CD34+ from SCD patients transduced in the presence or absence of UM171. Data represent mean ± SD, n = 8, each data point represents an individual mouse. *p < 0.05, **p < 0.01, ***p < 0.001.

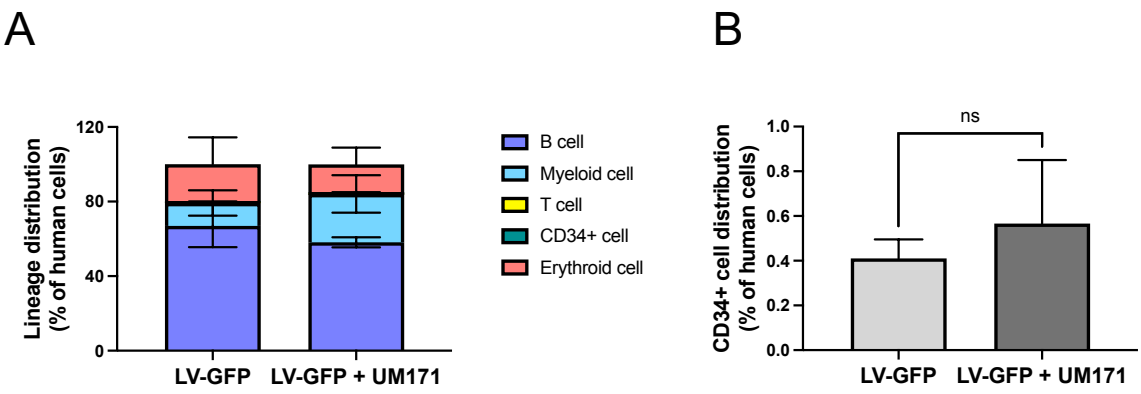


Figure S13. (A) Lineage distribution and (B) the percentage of CD34+ cells from SCD CD34+ transplanted BM human cells. Data represent mean ± SD, n = 6.

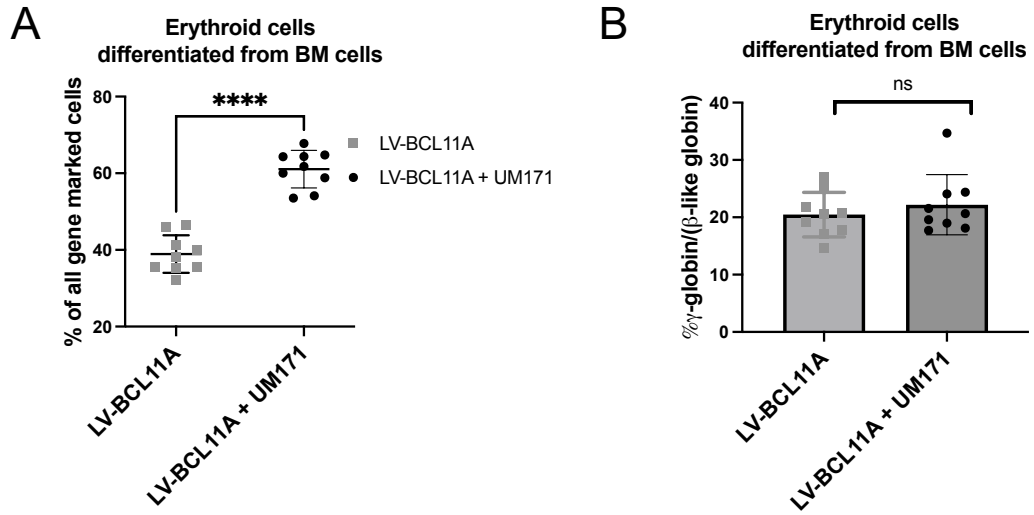


Figure S14. (A) Percentage of gene-marked cells after BM harvest and erythroid differentiation *in vitro*. (B) $\boldsymbol{\gamma}$-globin expression in gene-marked differentiated erythroid cells derived as in panel A. Data represent mean ± SD, n = 9, each data point represents an individual mouse. **** $p < 0.0001$.

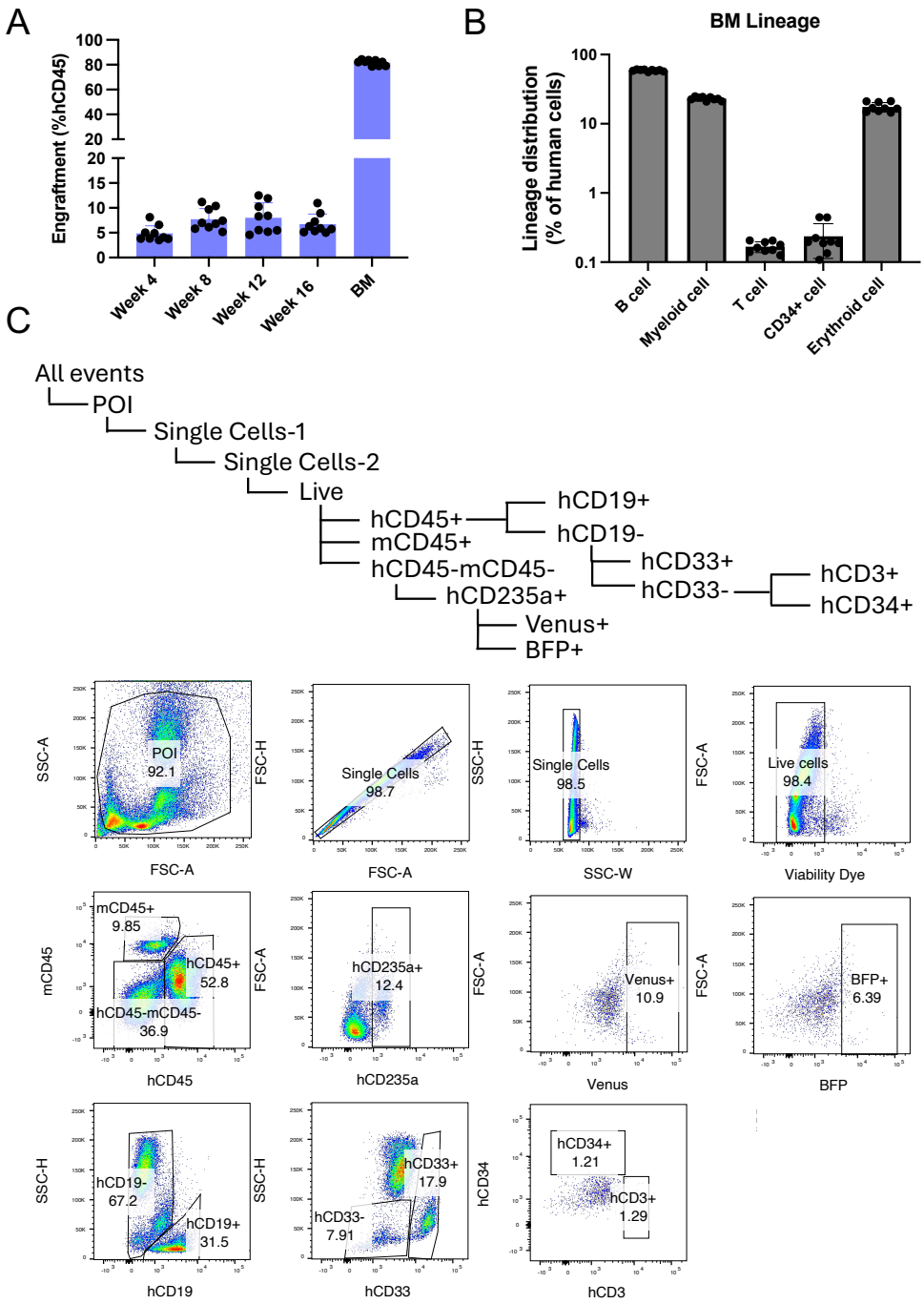


Figure S15. (A) Engraftment of CD34-derived hCD45+ cells in PB and BM in competitive assay. (B) Lineage distribution of SCD CD34+ transplanted BM human cells in competitive assay. (C) Representative flow cytometry analysis of bone marrow of mice after engraftment with human CD34+ cells. Hierarchy of FACS gates and representative plots for each gate are shown for a representative transplanted bone marrow sample. The first gate was plotted to delineate the cell population of interest (POI) and avoid debris. The second and third gates were plotted to exclude doublets. Values in plots are for respective gates.

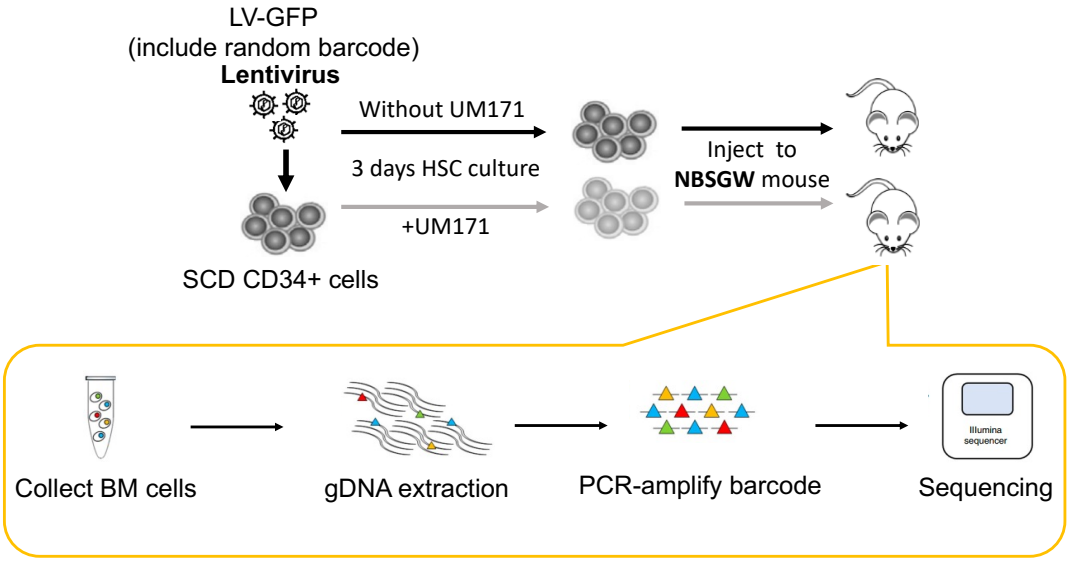


Figure S16. Schematic depiction of the barcoding strategy used for clonal tracking of CD34+ from SCD patients after transplantation and engraftment in NBSGW mice. CD34+ cells transduced with a LV-GFP vector containing a random barcode in presence or absence of UM171. NBSGW were transplanted with the transduced cells, and BM cells were collected at week 16. gDNA was extracted from the NBSGW BM, the barcode fragments were amplified by PCR and sequenced by the next generation sequencing as detailed in the materials and methods.

A

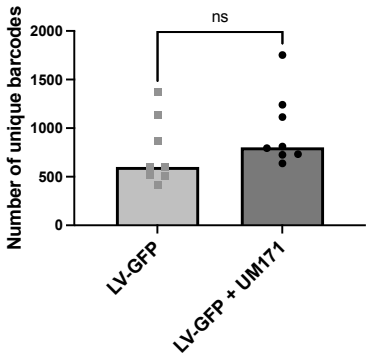


B

| | SCD P1 | SCD P2 | SCD P3 | SCD P4 | SCD P5 | SCD P6 | SCD P7 | SCD P8 |
|---|---|---|---|---|---|---|---|---|
| LV-GFP | 505 | 1368 | 515 | 414 | 602 | 866 | 600 | 1136 |
| LV-GFP + UM171 | 638 | 732 | 725 | 1114 | 794 | 810 | 1241 | 1752 |

Figure S17. (A) Summary of the number of unique clones from transplanted BM cells. (B) Number of unique clones from each SCD patient donor cells. At least two nucleotides needed to be different for data inclusion, and single reads were discarded. Each data point represents an individual mouse transplanted with different SCD patients' cells. Data represent median, n = 8, p = 0.23.